Long non-coding RNA HHIP-AS1 inhibits lung cancer epithelial-mesenchymal transition and stemness by regulating PCDHGA9

ZHUANZHUAN ZHOU, YANPING LAI, SHAN CAO, QIFANG ZHUO and HUIQIN TANG

Department of Respiratory and Critical Care Medicine, The Second Hospital of Tianjin Medical University, Tianjin 300211, P.R. China

Received January 6, 2021; Accepted June 10, 2021

DOI: 10.3892/mmr.2021.12485

Abstract. The aim of the present study was to investigate the effect of hedgehog-interacting protein antisense RNA 1 (HHIP-AS1) on epithelial-mesenchymal transition (EMT) and cellular stemness of human lung cancer cells by regulating the microRNA (miR)-153-3p/PCDHGA9 axis. Reverse transcription-quantitative PCR was used to compare the expression of HHIP-AS1 in lung cancer and adjacent normal lung tissues. In addition, the correlation of HHIP-AS1 with E-cadherin, Vimentin, N-cadherin and Twist1 was analyzed. HHIP-AS1 overexpression vector was transfected into lung cancer A549 and NCI-H1299 cell lines. Cell Counting Kit-8 and Transwell and clonogenic assays were used to detect the proliferation, invasion and clonogenesis of the lung cancer cells, respectively. The associations among HHIP-AS1, miR-153-3p and PCDHGA9 were predicted by bioinformatics analysis and verified by a dual-luciferase reporter system. The results showed that the expression of HHIP-AS1 in lung cancer tissues was significantly lower than that in normal tissues (P<0.001). HHIP-AS1 was positively correlated with E-cadherin and negatively correlated with Vimentin, N-cadherin and Twist1. HHIP-AS1 overexpression inhibited the proliferation, invasion and clonal formation of the A549 and NCI-H1299 cells. The luciferase reporter system verified that HHIP-AS1 could adsorb miR-153-3p and that PCDHGA9 was the target gene of miR-153-3p. A549 cells were transfected with HHIP-AS1 overexpression vector and miR-153-3p mimic, and the miR-153-3p mimic had a mitigating effect on HHIP-AS1 inhibition (P<0.001). In conclusion, HHIP-AS1 inhibits the EMT and stemness of lung cancer cells by regulating the miR-153-3p/PCDHGA9 axis. Thus, HHIP-AS1 may be a new potential target for lung cancer treatment.

Correspondence to: Dr Zhuanzhuan Zhou, Department of Respiratory and Critical Care Medicine, The Second Hospital of Tianjin Medical University, 23 Pingjiang Road, Hexi, Tianjin 300211, P.R. China
E-mail: z142622@126.com

Abbreviations: NSCLC, non-small-cell lung cancer; PCDHGA9, protocadherinγ subfamily A9; EMT, epithelial-mesenchymal transition; ZEB2, E-box binding homeobox 2; lncRNA, long non-coding RNA; HHIP-AS1, hedgehog-interacting protein antisense RNA 1; LUAD, lung adenocarcinoma

Key words: lung cancer, lncRNA, HHIP-AS1, microRNA-153-3p, PCDHGA9, EMT, cellular stemness

Introduction

Lung cancer is the most common malignancy worldwide (1). Globally, >1.6 million new cases of lung cancer, which account for 12.7% of all new cancer cases, are reported each year, making this cancer type the most lethal malignancy (2). In total, >1.4 million patients with lung cancer succumb to the disease each year, and this number accounts for 19% of all cancer-related deaths annually (3). Although the treatment of lung cancer has been improved in recent years, the 5-year survival rate of patients with lung cancer, especially those with advanced stages, remains extremely low (4). Local recurrence, lymph node metastasis and distant metastasis are the main causes of death (5-7).

Long non-coding RNAs (lncRNAs) refer to functional RNA molecules with transcriptional lengths of >200 nucleotides that are not translated into proteins (8,9). lncRNA is closely related to human health and disease (10-12). lncRNA plays an important role in the occurrence and development of tumors, including lung cancer (13,14). The lncRNA hedgehog-interacting protein antisense RNA 1 (HHIP-AS1) inhibits hepatocellular carcinoma progression by stabilizing hedgehog-interacting protein mRNA (15). However, the mechanism of HHIP-AS1 in lung adenoma has yet to be clarified. Thus, in the present study, the focus was on the role of HHIP-AS1 in the occurrence and development of lung cancer.

MicroRNAs (miRNAs/miRs) are highly conserved non-coding RNAs (16). miRNAs are involved in cell proliferation, apoptosis, cell differentiation and other biological behaviors by regulating the expression of corresponding genes. miRNAs can also be involved in the invasion and migration of malignant tumors, the regulation of the tumor microenvironment and the regulation of tumor stem cells (TSCs) (17,18). miR-153-3p is closely associated with tumor detection (19-21).

However, the mechanism of miR-153-3p in the development and progression of lung cancer is unclear.

Protocadherin (PCDH), as a member of the cadherin family, may play an important role in the establishment and function of specific cell-cell connections in the brain (22). The extracellular coding sequence of classical cadherin is interrupted by numerous introns (23). In comparison, the coding sequence of the corresponding part of PCDH does not contain introns (24). High levels of PCDH are produced in the brain in specific forms, but their function is unknown. At least one homophobic binding tendency has been observed in PCDH. This binding tendency is similar to that in classical cadherin (25). Little information is available on the relationship between PCDHs and tumorigenesis or nuclear signaling (26). Protocadherinγ subfamily A9 (PCDHGA9) is a potential new biomarker in gastric cancer and is closely associated with the outcome of patients with gastric cancer (27,28). However, to the best of our knowledge, the role and function of PCDHGA9 in lung cancer have not been reported.

The aim of the current study was to investigate the expression level of HHIP-AS1 in lung cancer tissues and adjacent tissues. HHIP-AS1 was overexpressed in A549 and NCI-H1299 cells. Changes in cell proliferation, invasion, epithelial-mesenchymal transition (EMT) and cellular stemness were then investigated. The associations between HHIP-AS1 and miR-153-3p and PCDHGA9 were further explored.

Materials and methods

Lung cancer tissue collection. A total of 20 patients, including 12 males and 8 females, aged between 54-82 years, (average age, 58.7±11.8 years) who were clinically and pathologically diagnosed with lung cancer and treated surgically between March and October 2020, were selected as the study subjects. Specimens were collected in the Department of Tumor Surgery of The Second Hospital of Tianjin Medical University. All patients met the following inclusion criteria: i) The selected specimens were pathologically confirmed as NSCLC and paracancer tissue; ii) All patients were not treated with radiotherapy or chemotherapy; and iii) Complete follow-up data of patients. Exclusion criteria included: Presence of other tumors or systemic diseases that threaten life and health. Cancer tissues and adjacent tissues (5 cm away from the cancer tissue) were collected. Patients with a preoperative history of chemotherapy were excluded.

All patients provided written informed consent. The present study was reviewed and approved by the Ethics Review Committee of the Second Hospital of Tianjin Medical University (Tianjin, China).

Cell culture. A549 and NCI-H1299 cell lines were obtained from the Cell Bank of the Chinese Academy of Sciences (Shanghai, China). The cells were cultured in DMEM containing 10% FBS (both Gibco; Thermo Fisher Scientific, Inc.). The cells were placed in an incubator at 37˚C with 5% CO_2. Logarithmic growth cells were collected. Cell passage was performed every 2 days.

Cell transfection. Cells in the logarithmic phase and in good growth condition were inoculated into a six-well plate a day before transfection. The cell density was 70-80% after 12 h of adherence to the cell-culture dish. Prior to transfection, the cells were replaced with a medium without penicillin-streptomycin mixed solution. Lipofectamine® 3000 (Thermo Fisher Scientific, Inc.) transfection reagent was added according to the instructions. The negative control (NC; empty vector, pcDNA3.1), pcDNA3.1-HHIP-AS1, pcDNA3.1-PCDHGA9, mimic-NC (5'-UUGUACUACACAAAAGUACUG-3'), miR-153-3p mimic (5'-TTGCATAGTCACAAAAGTGATC-3'), inhibitor-NC (5'-CAGUACUUUUGUGUAGUACAA-3') and miR-153-5p inhibitor (5'-GATCACTTTTGTGACTATGCAA-3') were purchased from Shanghai GeneChem Co., Ltd., and separately transfected into the cells. The culture medium was replaced with DMEM (10% FBS) after 8 h. Cells were transfected with 2 μg HHIP-AS1 vector (1 μg/ml), 40 nM miR-153-3p mimic and 20 nM miR-153-3p inhibitor. After the cells had been incubated at 37˚C for 48 h, further experimentation was performed.

Reverse transcription-quantitative (RT-q)PCR experiments. The cancer tissues and adjacent tissues were washed with 0.9% sodium chloride solution, placed into the RNA sample storage solution, and stored in a refrigerator at -80˚C. The total RNA of lung cancer tissue and cells was extracted with TRIzol® reagent (Invitrogen; Thermo Fisher Scientific, Inc.). The integrity of the total RNA was determined by electrophoresis. cDNA was reverse transcribed using the Prime Script™ 1st Strand cDNA Synthesis kit (Takara Bio, Inc.). The primer sequences are shown in Table I. The reaction system (20 μl) comprised 10 μl, 0.6 μl of upstream primer (10 μmol/l), 0.6 μl of downstream primer (10 μmol/l), 1 μl of cDNA and 7.8 μl of double distilled water. The reaction conditions were as follows: 95˚C for 10 min, 95˚C for 15 sec and 60˚C for 1 min (40 cycles). The coefficients of determination of the standard curves generated by the software were all >0.99, and the amplification efficiency was 90-110%. The $2^{-\Delta\Delta Cq}$ method was used to calculate the difference in gene expression (29).

Cell proliferation assay. The cells were inoculated into a 96-well plate at a density of $5x10^3$ cells/well. Fresh culture medium (90 μl) containing 10% FBS and 10 μl Cell Counting Kit-8 (CCK-8) solution (Dojindo Molecular Technologies, Inc.) was placed into each well. The CCK-8 assay was used according to the manufacturer's protocols. The reaction was then placed in an incubator at 37˚C with 5% CO_2 for 4 h. The optical density of each well at 450 nm was determined using an immunoplate reader. The average value of each group was used to reflect the proliferation ability of the cells.

Transwell invasion assay. All reagents and equipment were pre-cooled on ice. The Transwell chamber was placed in a 24-well plate, and 50 μl (0.2 μg/μl) of Matrigel (BD Biosciences) was evenly spread on the membrane of the Transwell chamber (MilliporeSigma). The precoating occurred at 37˚C and was left for 15 min to solidify. The cells were digested using 0.125% trypsin (37˚C, 5 min), centrifuged at 200 x g/min for 5 min at 4˚C, counted, and then diluted in serum-free medium to $2.5x10^4$ cells/ml to prepare a cell suspension. The cell suspension was added to the upper Transwell chamber at 200 μl/well, and 500 μl medium with 10% FBS was added to the lower Transwell chamber. The Transwell chamber was

Table I. Primer sequences for reverse transcription-quantitative PCR.

Gene	Forward primer (5'-3')	Forward primer (5'-3')
HHIP-AS1	GGCTGAAGAAGCAGAGGATAG	TTCACCACTCTGTCGGTTTAG
miR-153-3p	GGGTTGCATAGTCACAAAAG	TTTGGCACTAGCACATT
PCDHGA9	GCTCATTTCGGTGGAAGAT	CACTGGGCTAAACAGAGAT
N-cadherin	GGTGGAGGAGAAGAAGACCAG	GGCATCAGGCTCCACAGTG
Vimentin	GAGAACTTTGCCGTTGAAGC	GCTTCCTGTAGGTGGCAATC
Snail	CCTCCCTGTCAGATGAGGAC	CCAGGCTGAGGTATTCCTTG
Slug	GGGGAGAAGCCTTTTTCTTG	TCCTCATGTTTGTGCAGGAG
E-cadherin	TGCCCAGAAAATGAAAAAGG	GTGTATGTGGCAATGCGTTC
CD44	TTGCAGTCAACAGTCGAAGAAG	CCTTGTTCACCAAATGCACCA
Oct4	CTTGCTGCAGAAGTGGGTGGAGGAA	CTGCAGTGTGGGTTTCGGGCA
CD133	TGGATGCAGAACTTGACAACGT	ATACCTGCTACGACAGTCGTGGT
SOX2	GCCGATGTGAAACTTTTGTCG	GGCAGCGTGACTTATCCTTCT
GAPDH	TGCACCACCAACTGCTTAGC	GGCATGGACTGTGGTCATGAG
U6	CTCGCTTCGGCAGCACA	AACGCTTCACGAATTTGCGT

PCDHGA9, protocadherinγ subfamily; HHIP-AS1, hedgehog-interacting protein antisense RNA 1.

placed in a 37˚C incubator for culturing (48 h). The cells were fixed with 4% formaldehyde for 15 min at room temperature. Then, stained with 0.1% crystal violet for 15 min at room temperature. Next, the cells on the inner membrane were gently wiped with a cotton swab. The number of cells that had passed through the filter membrane was counted under a fluorescence microscope (Nikon Corporation) in four high-power fields (magnification, x40). The experiment was repeated three times.

Clonogenic analysis. Cells at a density of 200 cells/well were inoculated into a 12-well plate after 24 h of transfection. The cells were cultured in an incubator with 5% CO_2 at 37˚C. The liquid was changed every 2 days. After 15 days, the medium was discarded and 10% precooled methanol (4˚C) was used for fixation for 20 min. A total of 400 μl 1% crystal violet (Solarbio) was added to each well. The cells were stained at room temperature for 10 min and rinsed with water for 5 min. Cell clones were counted under a fluorescence microscope (Nikon Corporation).

Western blotting analysis. The transfected cells were collected and lysed with RIPA buffer (Beyotime Institute of Biotechnology), and total protein was extracted. Protein concentration was determined by the BCA method. Loading buffer was added to denatured protein. 12% SDS-PAGE was performed on 30 μg protein samples of each group. The cells were then transferred to PVDF membranes. Cells were then blocked using 5% skimmed milk powder (1X PBS) for 2 h at room temperature. Primary antibodies for E-cadherin (cat. no. ab40772, 1:1,000), Vimentin (cat. no. ab92547, 1:1,000), N-cadherin (cat. no. ab76011, 1:1,000), Snail1 (cat. no. ab216347, 1:1,000), Slug (cat. no. ab51772, 1:1,000), Twist1 (cat. no. ab50887, 1:1,000), Oct4 (cat. no. ab200834, 1:1,000), SOX2 (cat. no. ab171380, 1:1,000), CD44 (cat. no. ab189524, 1:1,000) and CD133 (cat. no. ab222782, 1:1,000) were added and incubated overnight at 4˚C. All antibodies were purchased from Abcam. HRP-labeled secondary antibodies (1:10,000, Thermo Fisher Scientific, Inc.; cat. nos. A16072 and A16104) were added and incubated at room temperature for 2 h. After washing in TBST (0.1% Tween-20; Thermo Fisher Scientific, Inc.), cells were developed in ECL solution (MilliporeSigma; cat. no. MA01821). The images were exposed and analyzed using a Bio-Rad gel imaging system.

Online database analysis. In this study, two database websites, StarBase (version: v2.0; http://starbase.sysu.edu.cn/) (30) and TargetScan (version: 7.1; http://www.targetscan.org/vert_71/) (31), were used simultaneously. The binding sites of HHIP-AS1 and miR-153-3p were analyzed through StarBase. The binding sites of miR-153-3p and PCDHGA9 were analyzed by TargetScan. The Cancer Genome Atlas data were used to analyze the expression of PCDHGA9 in lung adenocarcinoma (LUAD) tissues and normal tissues. Data were obtained from the UALCAN website (http://ualcan.path.uab.edu/analysis.html) (32). Immunohistochemical images of PCDHGA9 were downloaded from The Human Protein Atlas (https://www.proteinatlas.org/) website (33).

Double luciferase reporter gene detection experiment. The pmirGLO dual-luciferase reporter gene detection system from Promega Corporation was used. The 3'-untranslated regions of HHIP-AS1 and PCDHGA9 and the sequence fragments of the binding site of miR-153-3p were chemically synthesized. The pmirGLO luciferase expression vector (Promega Corporation) was inserted to obtain the wild-type vectors, pmirGLO/HHIP-AS1-wt and pmirGLO/PCDHGA9-wt. The mutant sequence was synthesized in the same way to obtain the mutant vectors pmirGLO/HHIP-AS1-mt and pmirGLO/PCDHGA9-mt. pmirGLO/HHIP-AS1-wt, pmirGLO/PCDHGA9-wt, pmirGLO/HHIP-AS1-mt, pmirGLO/PCDHGA9-mt, miR-153-3p mimic and the

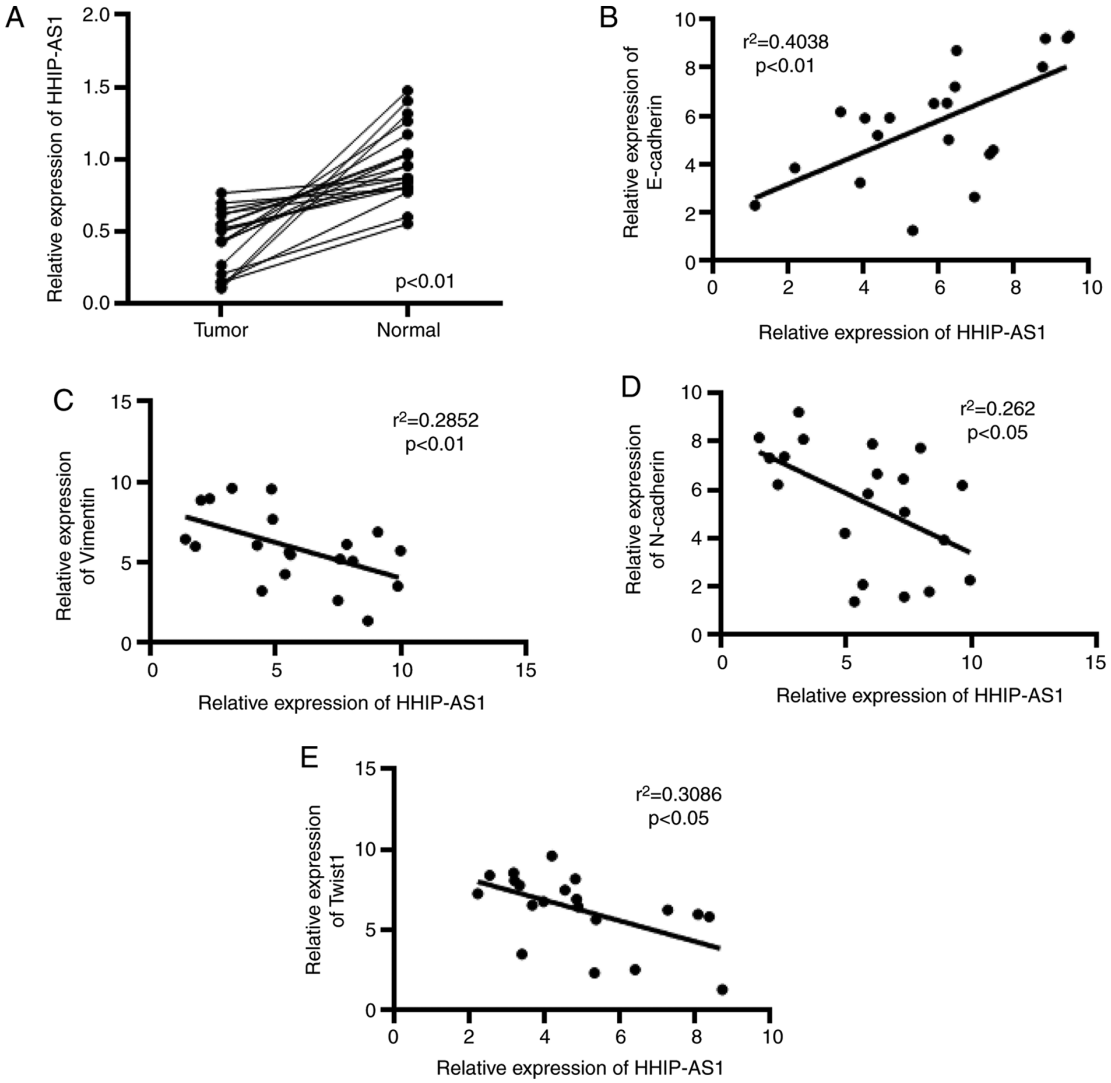

Figure 1. Low expression of HHIP-AS1 in lung cancer. (A) The expression level of HHIP-AS1 in lung cancer tissues was lower than that of adjacent tissues. (B) The expression level of HHIP-AS1 was positively correlated with the expression level of E-cadherin. (C) The expression of HHIP-AS1was negatively correlated with the expression of Vimentin. (D) HHIP-AS1 expression was negatively correlated with N-cadherin expression. (E) HHIP-AS1 expression was negatively correlated with Twist1 expression. Error bars represent the mean ± SD values. HHIP-AS1, hedgehog-interacting protein antisense RNA 1.

mimics-NC were separately mixed with Lipofectamine 3000 for cell transfection. The cells were collected after 48 h of transfection, as per the instructions of the dual luciferase reporter gene kit, and *Renilla* was used as the internal reference. A total of 150 μl 1X lysis buffer PLB was added to each well of 24-well plate to cover cells, following which they were completely lysed. Then, 50 μl LAR II was added to 1.5 ml EP tubes. Next, 10 μl cell lysate was added to the 1.5 ml EP tube containing LAR II, the solution was then mixed and placed in detector for analysis. After the measurement, the EP tube was removed and 50 μl Stop & GloR reagent was added and mixed, following which it was placed in the detector again (Promega Corporation). The ratio of the fluorescence value of the luciferase to the fluorescence value of the *Renilla* was calculated, and the relative viability of the reporter gene in the cell was evaluated.

Statistical analysis. SPSS19.0 software (IBM Corp.) was used for statistical processing. Each set of experiments was repeated three times. Measurement data are expressed as the mean ± SD. The paired Student's t-test was used in Figs. 1A and 6A. The other data with two groups were compared using unpaired Student's t-test. One-way ANOVA followed by Tukey's multiple comparisons test was used for the comparisons among groups. Spearman's correlation analysis was used for assessing the correlation between expression levels. P<0.05 was considered to indicate a statistically significant difference.

Results

HHIP-AS1 is poorly expressed in lung cancer. In this study, the expression of HHIP-AS1 in lung cancer tissues and adjacent tissues was first measured. The detection results showed that the expression level of HHIP-AS1 in lung cancer tissues was decreased compared with that in adjacent tissues (Fig. 1A). The correlation of HHIP-AS1 with E-cadherin, Vimentin, N-cadherin and Twist1 was also analyzed. The experimental results showed that the expression of HHIP-AS1 and E-cadherin was positively correlated (Fig. 1B), whereas HHIP-AS1 was negatively correlated with Vimentin, N-Cadherin and Twist1 (Fig. 1C-E).

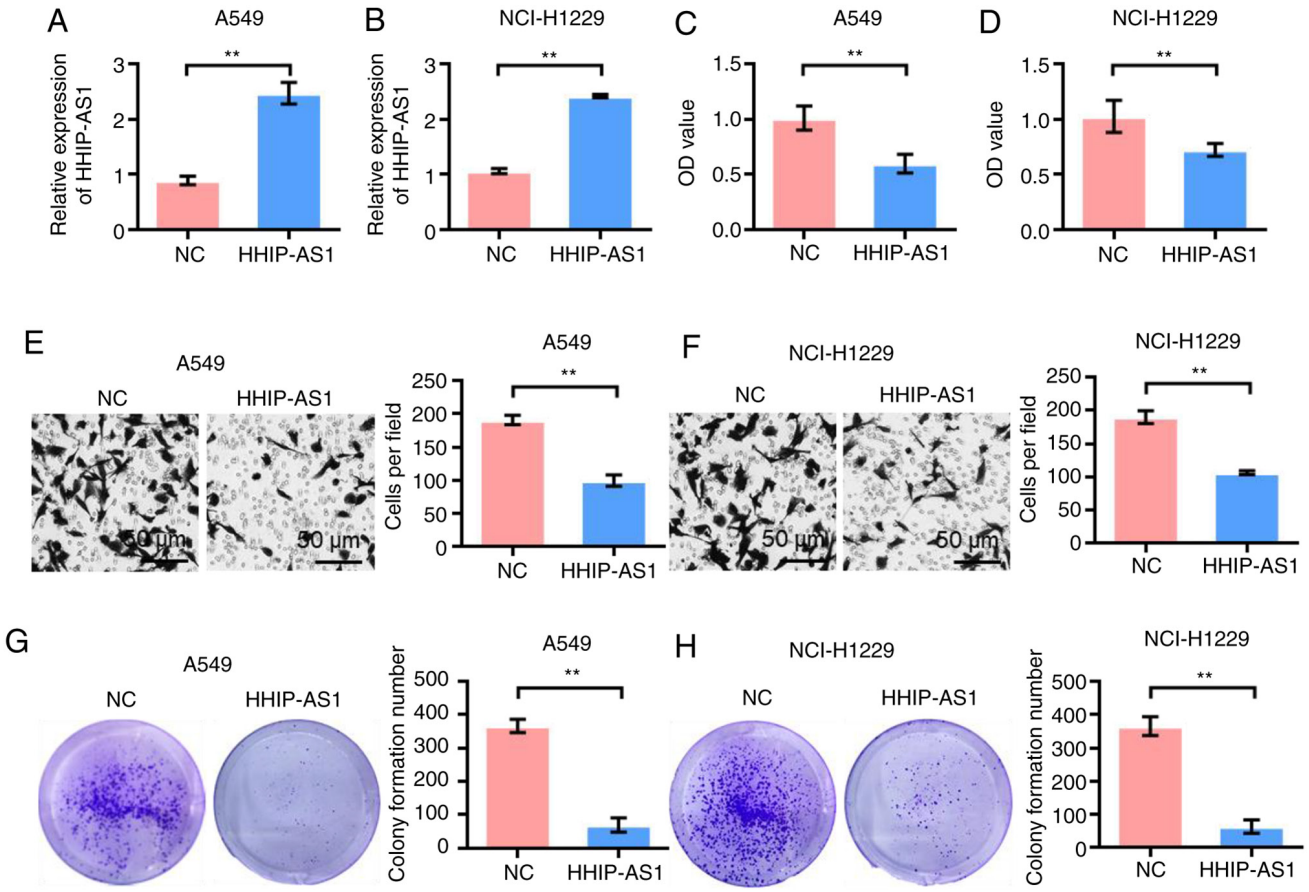

Figure 2. Overexpression of HHIP-AS1 inhibits lung cancer proliferation, invasion and clone formation. (A) Detection of the efficiency of overexpression of HHIP-AS1 in A549 cells. The results showed that the overexpressed plasmid could upregulate the expression of HHIP-AS1. (B) Detection of the efficiency of overexpression of HHIP-AS1 in NCI-H1299 cells. Overexpression of HHIP-AS1 inhibited the proliferation of (C) A549 and (D) NCI-H1299 cells. Overexpression of HHIP-AS1 inhibited the invasion of (E) A549 and (F) NCI-H1299 cells. Overexpression of HHIP-AS1 inhibited the colony formation ability of (G) A549 and (H) NCI-H1299 cells. Error bars represent the mean ± SD values. **P<0.01. HHIP-AS1, hedgehog-interacting protein antisense RNA 1; NC, negative control.

HHIP-AS1 overexpression inhibits the proliferation, invasion and clonal formation of lung cancer cells. The effect of HHIP-AS1 overexpression on lung cancer cell lines was studied to investigate its biological role. First, the transfection efficiency of overexpressing HHIP-AS1 in A549 and NCI-H1299 cells was detected. The experimental results showed that the expression of HHIP-AS1 was higher in the HHIP-AS1 transfection group than that in the NC group (pcDNA3.1-NC) after pcDNA3.1-HHIP-NC was transfected into the A549 and NCI-H1299 cell lines (P<0.01; Fig. 2A and B). The CCK-8 results showed that the proliferation of the A549 and NCI-H1299 cells was significantly lower after HHIP-AS1 overexpression compared with that of the control group (P<0.01; Fig. 2C and D). The Transwell test results showed that the invasion ability of the A549 and NCI-H1299 cells was significantly lower after HHIP-AS1 overexpression than that in the control group (P<0.01; Fig. 2E and F). The results of the clonal formation experiment showed that the number of colony formations of A549 and NCI-H1299 cell lines overexpressing HHIP-AS1 was significantly lower than that of the control group (P<0.01; Fig. 2G and H).

HHIP-AS1 overexpression inhibits the EMT and cell stemness of lung cancer cells. The effect of HHIP-AS1 overexpression on EMT and stem cell markers in lung cancer cells was examined. RT-qPCR analysis confirmed that the overexpression of the HHIP-AS1 gene significantly increased the expression of the epithelial marker, E-cadherin (P<0.01; Fig. 3A) and decreased the expression of mesenchymal markers (Fig. 3B-F). RT-qPCR analysis showed that the upregulation of HHIP-AS1 significantly reduced the expression of stemness-related genes Oct4 and SOX2 (Fig. 3G and H) and CD44- and CD133-related surface antigens in cancer stem cells (P<0.01; Fig. 3I and J). In order to further verify the role of lncRNA HHIP-AS1, changes in the expression levels of E-cadherin, Vimentin, N-cadherin, Snail1, Slug, Twist1, Oct4, SOX2, CD44 and CD133 after the overexpression of HHIP-AS1 were identified using western blot analysis. The results showed that overexpression of HHIP-AS1 increased the expression of the epithelial marker E-cadherin. However, overexpression of HHIP-AS1 inhibited the expression of the mesenchymal marker Vimentin and N-cadherin. In addition, after overexpression of HHIP-AS1, the expression levels of Snail1, Slug, Twist1, Oct4, SOX2, CD44 and CD133 were also downregulated (Fig. 3K-L).

miR-153-3p is the target gene of HHIP-AS1. Bioinformatics analysis was performed using the StarBase database (http://starbase.sysu.edu.cn/) to predict the binding sites of miR-153-3p and HHIP-AS1 (Fig. 4A). Further experiments showed that HHIP-AS1 overexpression inhibited the expression of miR-153-3p (Fig. 4B).

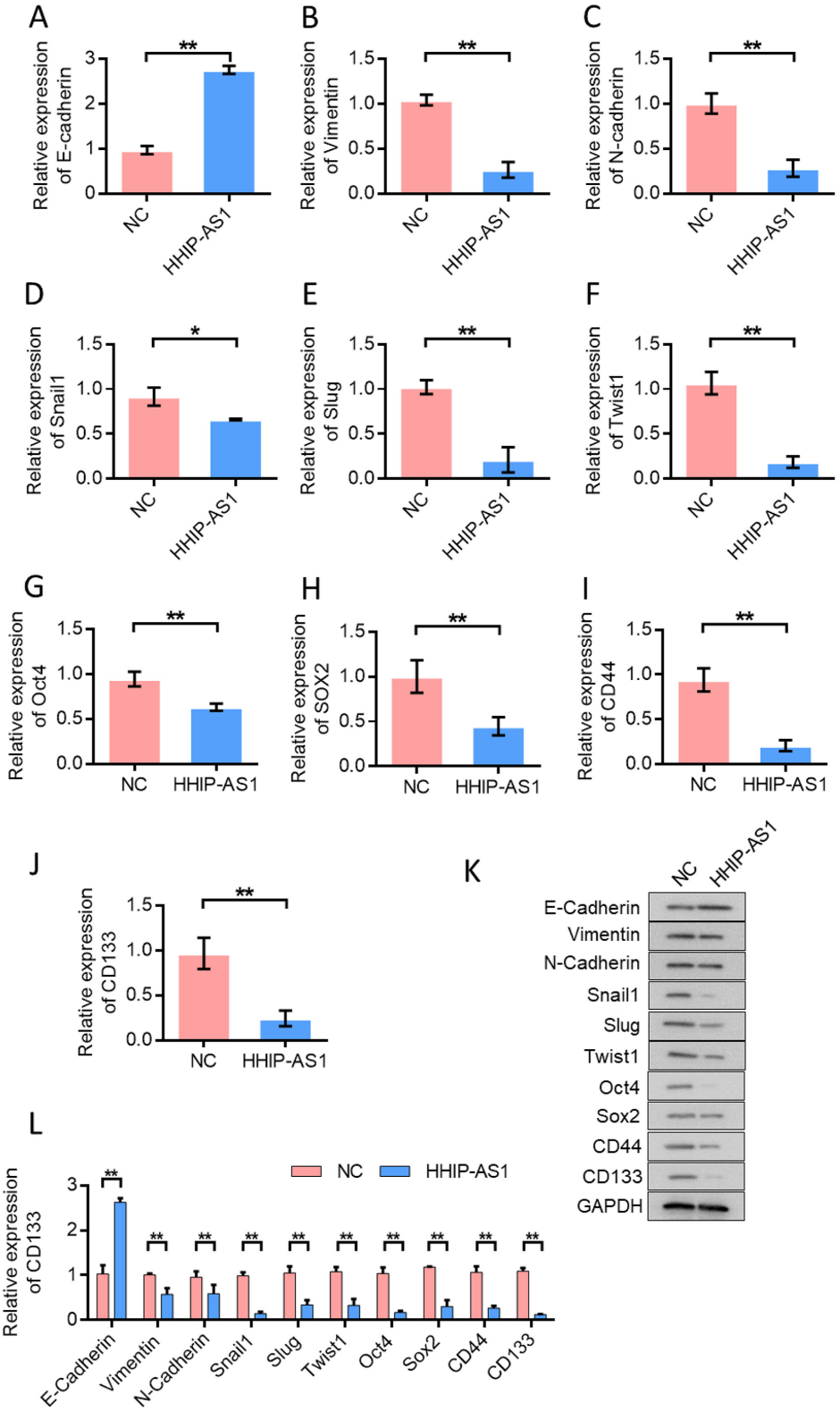

Figure 3. Overexpression of HHIP-AS1 inhibits EMT and cell stemness of lung cancer cells. (A) Detection of E-cadherin expression in lung cancer cells. Overexpression of HHIP-AS1 upregulated the expression of E-cadherin. Detection of (B) Vimentin, (C) N-cadherin, (D) Snail1, (E) Slug, (F) Twist1, (G) Oct4, (H) SOX2, (I) CD44and (J) CD133 expression in lung cancer cells. (K) Western blotting detected the changes in the expression levels of E-cadherin, Vimentin, N-cadherin, Snail1, Slug, Twist1, Oct4, SOX2, CD44 and CD133 after the overexpression of HHIP-AS1. (L) The semi-quantification for the western blotting results. Error bars represent the mean ± SD values. *P<0.05, **P<0.01. HHIP-AS1, hedgehog-interacting protein antisense RNA 1; NC, negative control.

The pmirGLOdual-luciferase reporter system was used for further verification. The results showed that miR-153-3p could inhibit the luciferase expression of wild-type HHIP-AS1 (P<0.01). However, the inhibitory effect disappeared when the HHIP-AS1 binding site was mutated (Fig. 4C). The double luciferase reporter gene assay showed that HHIP-AS1 could adsorb miR-153-3p. The correlation test results of miR-153-3p and HHIP-AS1 expression showed a negative correlation (Fig. 4D).

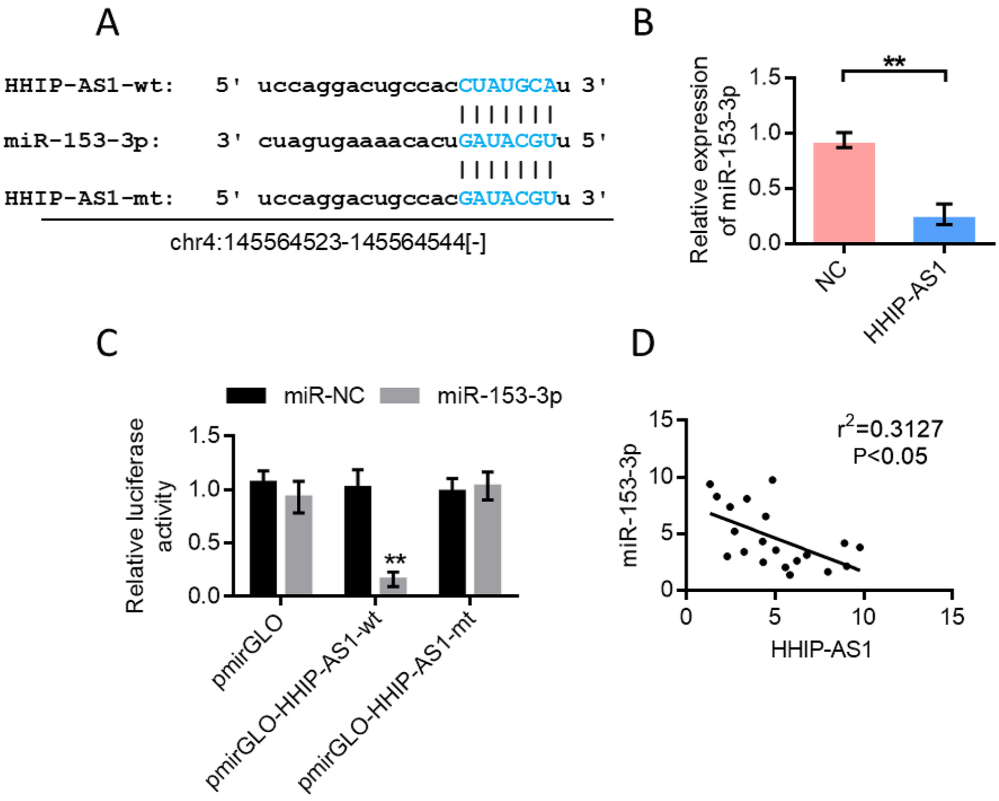

Figure 4. miR-153-3p is the target gene of HHIP-AS1. (A) Schematic diagram of the binding site of miR-153-3p and HHIP-AS1. (B) Overexpression of HHIP-AS1 inhibited the expression of miR-153-3p. (C) The dual luciferase reporter gene detection experiment verified the binding of miR-153-3p and HHIP-AS1. (D) The expression of miR-153-3p and HHIP-AS1 was negatively correlated. Error bars represent the mean ± SD values. **P<0.01. HHIP-AS1, hedgehog-interacting protein antisense RNA 1; NC, negative control; miR, microRNA; wt, wild-type; mt, mutant.

miR-153-3p directly targets PCDHGA9 in lung cancer. TargetScan (http://www.targetscan.org/vert_72/) predicted that miR-153-3p could bind to PCDHGA9. Fig. 5A shows the schematic diagram of the binding site of miR-153-3p with PCDHGA9. The RT-qPCR results showed that overexpression of miR-153-3p inhibited the expression of PCDHGA9 (Fig. 5B and C). Subsequently, the pmirGLOdual-luciferase reporter system was used for further verification. The results showed that miR-153-3p inhibited the luciferase expression of wild-type PCDHGA9 (P<0.01). However, the inhibitory effect disappeared when the binding site of PCDHGA9 was mutated (Fig. 5D). The correlation test results of miR-153-3p and PCDHGA9 expression showed a negative correlation (Fig. 5E). The expression of PCDHGA9 in 515 patients with lung cancer was lower and the difference was statistically significant (Fig. 5F), based on data from The Cancer Genome Atlas (http://ualcan.path.uab.edu/analysis.html).Transfection experiments using PCDHGA9 expression vector and PCDHGA9 + miR-153-3p mimic were performed. CCK-8 was used to detect the change in cell proliferation ability after different treatments. The transfection efficiency results for the overexpression of PCDHGA9 are provided in Fig. 5G. The results showed that the proliferation ability of A549 and NCI-H1299 cells was decreased after PCDHGA9 overexpression compared with the control group. However, cell proliferation ability was enhanced by the simultaneous transfection of PCDHGA9 overexpression plasmid and miR-153-3p mimic compared with the PCDHGA9 overexpression group (Fig. 5H-K).

PCDHGA9 expression mediates the biological effect of HHIP-AS1. The Human Proteins Atlas database (http://www.proteinatlas.org/) in data analysis was employed and the results showed that PCDHGA9 was decreased in LUAD tissue compared with normal lung tissue (Fig. 6A) (33). Immunohistochemical images of PCDHGA9 were downloaded from The Human Protein Atlas (https://www.proteinatlas.org/ENSG00000261934-PCDHGA9/pathology/lung+cancer) website. Subsequently, PCDHGA9 expression was detected in A549 and NCI-H1299 cells after different transfections. The results showed that HHIP-AS1 overexpression upregulated the expression of PCDHGA9. However, miR-153-3p overexpression inhibited the expression of PCDHGA9. A549 and NCI-H1299 cells were simultaneously transfected with HHIP-AS1 overexpression vector and miR-153-3p, and the result showed that miR-153-3p could reverse the effect of HHIP-AS1 (Fig. 6B and C). Cell proliferation and invasion experiments showed that HHIP-AS1 overexpression could inhibit the proliferation and invasion of A549 and NCI-H1299 cells. miR-153-3p overexpression promoted cell proliferation and invasion. A549 and NCI-H1299 cells were simultaneously transfected with HHIP-AS1 overexpression vector and miR-153-3p, and the results showed that miR-153-3p could reverse the anticancer effect of HHIP-AS1 (Fig. 6D-G).

Discussion

Tumor invasion and metastasis are the main causes of death in patients with lung cancer (34). The manner in which to

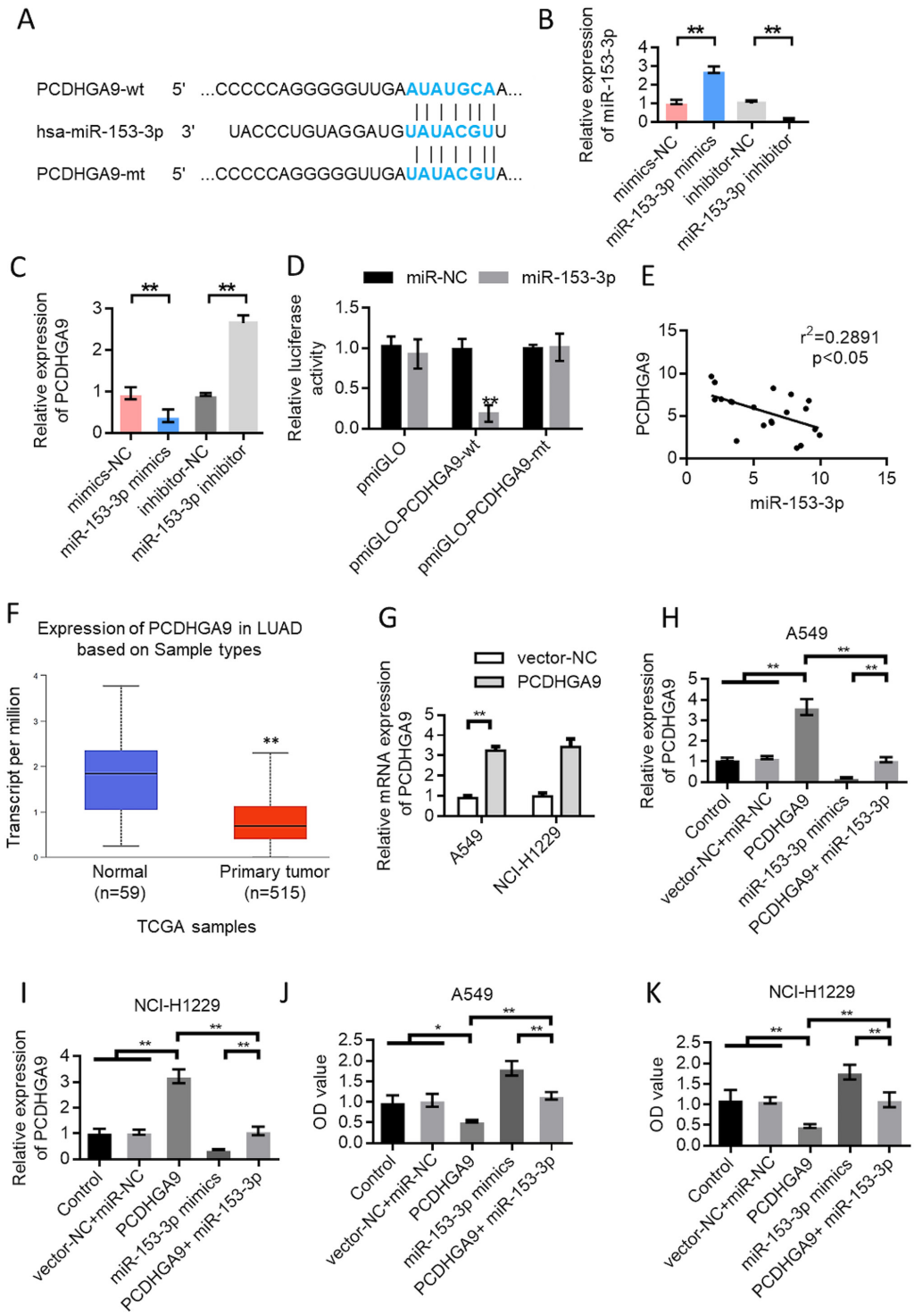

Figure 5. In lung cancer, miR-153-3p directly targets PCDHGA9. (A) Schematic diagram of the binding site of miR-153-3p and PCDHGA9. (B) Verification of the transfection efficiency of miR-153-3p mimics. (C) Overexpression of miR-153-3p inhibited the expression of PCDHGA9. (D) The dual luciferase reporter gene detection experiment verified the binding of miR-153-3p to PCDHGA9. (E) The expression of miR-153-3p and PCDHGA9 was negatively correlated. (F) TCGA data were used to analyze the expression of PCDHGA9 in LUAD tissues and normal tissues. Data from UALCAN website (http://ualcan.path.uab.edu/analysis.html). (G) The transfection efficiency results for the overexpression of PCDHGA9.After transfection with PCDHGA9 expression vector and PCDHGA9+miR-153-3p mimics', the expression level of PCDHGA9 in (H) A549 and (I) NCI-H1299 cells was detected. After transfection with PCDHGA9 expression vector and PCDHGA9+miR-153-3p mimics, the cell proliferation ability of (J) A549 and (K) NCI-H1299 cells was detected. Error bars represent the mean ± SD values. *P<0.05, **P<0.01. HHIP-AS1, hedgehog-interacting protein antisense RNA 1; NC, negative control; miR, microRNA; wt, wild-type; mt, mutant; PCDHGA9, protocadherinγ subfamily A9; LUAD, lung adenocarcinoma.

inhibit the growth of lung cancer cells and block the invasion and metastasis of cancer cells remains an urgent issue to address (35). EMT is a process in which epithelial cells are transformed into mesenchymal cells and gain mesenchymal properties (36). EMT can enable epithelial tumor cells to acquire a mesenchymal phenotype and further enhance the invasion and metastatic abilities of tumor cells to obtain self-renewal ability and other stem-like characteristics. EMT

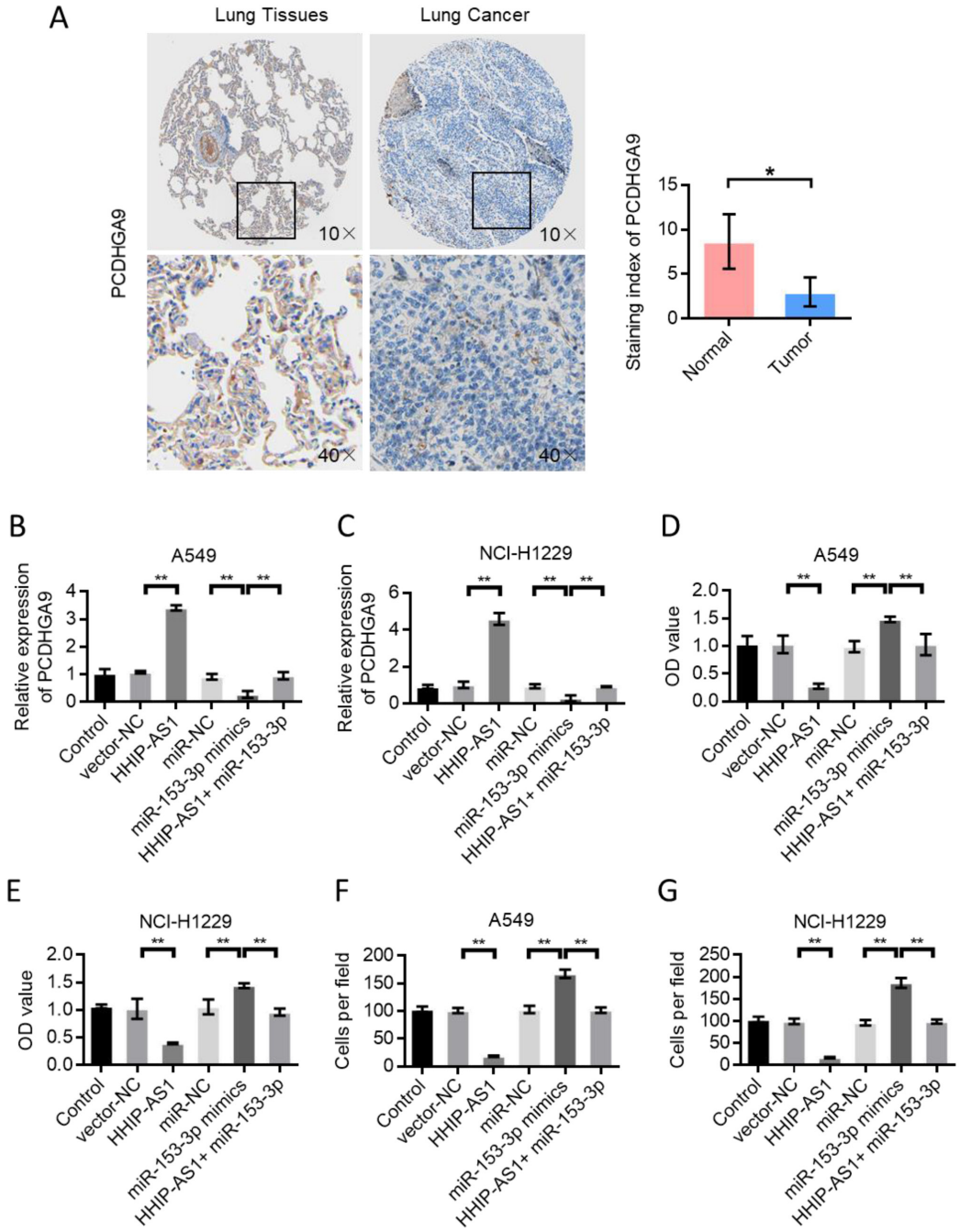

Figure 6. PCDHGA9 expression mediates the biological effects of long non-coding RNA HHIP-AS1. (A) Detection of PCDHGA9 expression in lung cancer tissues and adjacent tissues. Immunohistochemical results from The Human Proteins Atlas database (http://www.proteinatlas.org/). Detection of PCDHGA9 expression in (B) A549 and (C) NCI-H1299 cells after different treatments. After different treatments, cell proliferation of (D) A549 and (E) NCI-H1299 was detected. After different treatments, cell invasion of (F) A549 and (G) NCI-H1299 was detected. Error bars represent the mean ± SD values. *P<0.05, **P<0.01. HHIP-AS1, hedgehog-interacting protein antisense RNA 1; NC, negative control; miR, microRNA; PCDHGA9, protocadherinγ subfamily A9.

promotes the ability of tumor cells to acquire stem cell properties; thus, making tumor therapy more difficult (37-41).

Evidence shows that lncRNAs are involved in the self-renewal of embryonic and pluripotent stem cells, but whether lncRNAs drive the stem cell transformation process and their role in maintaining stem cell stemness are still unknown (42). Therefore, a better understanding of the molecular regulatory mechanisms and pathways of lncRNA in tumorigenesis provides a guarantee for the establishment of new treatment strategies and more effective cancer treatment methods (43). HHIP-AS1 is widely involved in tumor development. HHIP-AS1 inhibits the progression of hepatocellular carcinoma by stabilizing HHIP mRNA (15). However, it has also been reported that in Hedgehog (Hh)-driven human brain tumors, HHIP-AS1 promotes tumor survival by stabilizing the dynein complex 1 (15). In addition, HHIP-AS1 plays an important role in oncogenesis driven by the Sonic Hh pathway, an attractive therapeutic target (15). Thus, HHIP-AS1 can regulate cell proliferation and metastasis in a variety of tumors. Exploring the mechanism of HHIP-AS1 in inhibiting EMT and stem cell function in lung cancer is of great importance.

The mechanism of action of lncRNA is complex. One of its important mechanisms is to bind miRNA as a molecular

sponge to inhibit its silencing effect on the corresponding target mRNA downstream (44). A retrieval of TargetScan online bioinformatics indicated that miR-153-3p may be one of the binding molecules of HHIP-AS1 (45). Thus, we speculated that the anti-lung cancer cell effect of HHIP-AS1 may be realized through the adsorption of miR-153-3p. This hypothesis was verified through the overexpression of HHIP-AS1 in A549 cells. RT-qPCR detection showed that HHIP-AS1 overexpression markedly inhibited the expression level of miR-153-3p in A549 cells. TargetScan analysis indicated that *PCDHGA9* was the downstream inhibition target of miR-153-3p. The present study preliminarily indicated that the mechanism of action of HHIP-AS1 is the adsorption of miR-153-3p and the release of the inhibitory effect on PCDHGA9. The dual-luciferase reporter system was used to further verify the targeted relationship between miR-153-3p and PCDHGA9. lncRNA can regulate the expression of target genes through competing endogenous RNAs (ceRNAs). In the present study, it was found that HHIP-AS1 could target miR-153-3p and regulate the expression of PCDHGA9. HHIP-AS1/miR-153-3p/PCDHGA9 constituted the regulatory mechanism of ceRNA. *PCDHGA9*, as a tumor suppressor gene, can regulate the expression of E-cadherin. In the present study, the overexpression of PCDHGA9 upregulated the expression of E-cadherin.

EMT is essential for the maintenance of stem cell identity (46). Multipotent transcription factors, such as Oct4, Sox2, Fascin1 and Nanog, are highly expressed in TSCs ($CD133^+$ side population cells) (47). Transcription factors inhibits the expression of E-cadherin by acting on EMT-related regulatory factors and increases the expression levels of N-cadherin, E-box-binding homeobox 2 and Vimentin (48). These regulatory factors promote the occurrence of EMT and thus promote the invasion, metastasis and self-renewal of stem cells. The results of the present study showed that HHIP-AS1 inhibited the expression of stem cell markers. HHIP-AS1 can target Oct4, Sox2 and Nanog to decrease the sphere formation efficiency and colony formation of lung cancer cells. In addition, HHIP-AS1 upregulated the expression of epithelial markers while inhibiting the expression of mesenchymal markers. Thus, HHIP-AS1 can inhibit the EMT of lung cancer.

PCDHGA9 can induce autophagy, apoptosis and cell cycle arrest in gastric cancer cells, and inhibit EMT through the TGF-β/Smad2/3 pathway (27). In addition, PCDHGA9 overexpression in gastric cancer cells can enhance the expression of E-cadherin and decrease the expression of N-cadherin, Vimentin, Slug and Twist. PCDHGA9 knockdown has the opposite effect (28). Slug and Twist are key transcription factors in EMT. In the present study, HHIP-AS1 expression inhibited the expression of Slug and Twist by regulating the expression of PCDHGA9. HHIP-AS1 upregulated the expression of E-cadherin. These two factors are important for EMT in lung cancer progression. Cadherin downregulation leads to the disruption of cell-cell junctions, which is a key step in EMT that promotes tumor metastasis. PCDHGA9 is a member of the cadherin family, and PCDHGA9 overexpression can upregulate the expression of E-cadherin. The expression of Vimentin decreased after the overexpression of PCDHGA9. PCDHGA9 interacts directly with β-catenin and weakens the EMT-induced effect of the TGF-β and Wnt/β-catenin pathways (28). Therefore, PCDHGA9 inhibits EMT. This effect may also be the downstream molecular mechanism of PCDHGA9 regulated by HHIP-AS1 in targeting miR-153-3p.

In summary, HHIP-AS1 expression was decreased in lung cancer tissues. Mechanism of action studies have shown that HHIP-AS1 exerts an antitumor effect by inhibiting the EMT and cellular stemness of lung cancer cells through the adsorption of miR-153-3p and the inhibition of PCDHGA9 expression. As a new molecule closely related to lung cancer, HHIP-AS1 is a potential target for lung cancer treatment.

Acknowledgements

Not applicable.

Funding

No funding was received.

Availability of data and materials

The datasets used and/or analyzed in the current study are available from the corresponding author on reasonable request.

Authors' contributions

ZZ and HT designed the experiments and were responsible for confirming the authenticity of the raw data. ZZ and YL performed the experiments and data analysis. ZZ, SC, QZ and HT performed data analysis of cell experiments and wrote the manuscript, with contributions from all authors. All authors have read and approved the final manuscript.

Ethics approval and consent to participate

Clinical sample collection was approved by the Ethics Committee of The Second Hospital of Tianjin Medical University, and all patients provided written informed consent.

Patient consent for publication

Not applicable.

Competing interests

The authors declare that they have no competing interests.

References

1. Howlader N, Forjaz G, Mooradian MJ, Meza R, Kong CY, Cronin KA, Mariotto AB, Lowy DR and Feuer EJ: The effect of advances in lung-cancer treatment on population mortality. N Engl J Med 383: 640-649, 2020.
2. de Groot PM, Wu CC, Carter BW and Munden RF: The epidemiology of lung cancer. Transl Lung Cancer Res 7: 220-233, 2018.
3. Herbst RS, Morgensztern D and Boshoff C: The biology and management of non-small cell lung cancer. Nature 553: 446-454, 2018.
4. Oudkerk M, Devaraj A, Vliegenthart R, Henzler T, Prosch H, Heussel CP, Bastarrika G, Sverzellati N, Mascalchi M, Delorme S, *et al*: European position statement on lung cancer screening. Lancet Oncol 18: e754-e766, 2017.
5. Hirsch FR, Scagliotti GV, Mulshine JL, Kwon R, Curran WJ Jr, Wu YL and Paz-Ares L: Lung cancer: Current therapies and new targeted treatments. Lancet 389: 299-311, 2017.

6. Xi X, Liu N, Wang Q, Chu Y, Yin Z, Ding Y and Lu Y: ACT001, a novel PAI-1 inhibitor, exerts synergistic effects in combination with cisplatin by inhibiting PI3K/AKT pathway in glioma. Cell Death Dis 10: 757, 2019.
7. Zhong W, Hou H, Liu T, Su S, Xi X, Liao Y, Xie R, Jin G, Liu X, Zhu L, *et al*: Cartilage oligomeric matrix protein promotes epithelial-mesenchymal transition by interacting with transgelin in colorectal cancer. Theranostics 10: 8790-8806, 2020.
8. Sanli O, Dobruch J, Knowles MA, Burger M, Alemozaffar M, Nielsen ME and Lotan Y: Bladder cancer. Nat Rev Dis Primers 3: 17022, 2017.
9. Li K, Sun D, Gou Q, Ke X, Gong Y, Zuo Y, Zhou JK, Guo C, Xia Z, Liu L, *et al*: Long non-coding RNA linc00460 promotes epithelial-mesenchymal transition and cell migration in lung cancer cells. Cancer Lett 420: 80-90, 2018.
10. Liao J, Wang J, Liu Y, Li J and Duan L: Transcriptome sequencing of lncRNA, miRNA, mRNA and interaction network constructing in coronary heart disease. BMC Med Genomics 12: 124, 2019.
11. Li Y, Zhu G, Ma Y and Qu H: LncRNA CCAT1 contributes to the growth and invasion of gastric cancer via targeting miR-219-1. J Cell Biochem 120: 19457-19468, 2019.
12. Li P, Zhang N, Ping F, Gao Y and Cao L: lncRNA SCAL1 inhibits inducible nitric oxide synthase in lung cells under high-glucose conditions. Exp Ther Med 18: 1831-1836, 2019.
13. Wang S, Ke H, Zhang H, Ma Y, Ao L, Zou L, Yang Q, Zhu H, Nie J, Wu C, *et al*: LncRNA MIR100HG promotes cell proliferation in triple-negative breast cancer through triplex formation with p27 loci. Cell Death Dis 9: 805, 2018.
14. Tian T, Wang M, Lin S, Guo Y, Dai Z, Liu K, Yang P, Dai C, Zhu Y, Zheng Y, *et al*: The impact of lncRNA dysregulation on clinicopathology and survival of breast cancer: A systematic review and meta-analysis. Mol Ther Nucleic Acids 12: 359-369, 2018.
15. Bo C, Li X, He L, Zhang S, Li N and An Y: A novel long noncoding RNA HHIP-AS1 suppresses hepatocellular carcinoma progression through stabilizing HHIP mRNA. Biochem Biophys Res Commun 520: 333-340, 2019.
16. Xi X, Chu Y, Liu N, Wang Q, Yin Z, Lu Y and Chen Y: Joint bioinformatics analysis of underlying potential functions of hsa-let-7b-5p and core genes in human glioma. J Transl Med 17: 129, 2019.
17. Pipan V, Zorc M and Kunej T: MicroRNA polymorphisms in cancer: A literature analysis. Cancers (Basel) 7: 1806-1814, 2015.
18. Wong HA, Fatimy RE, Onodera C, Wei Z, Yi M, Mohan A, Gowrisankaran S, Karmali P, Marcusson E, Wakimoto H, *et al*: The Cancer Genome Atlas analysis predicts microRNA for targeting cancer growth and vascularization in glioblastoma. Mol Ther 23: 1234-1247, 2015.
19. Li L, Wang M, Mei Z, Cao W, Yang Y, Wang Y and Wen A: lncRNAs HIF1A-AS2 facilitates the up-regulation of HIF-1α by sponging to miR-153-3p, whereby promoting angiogenesis in HUVECs in hypoxia. Biomed Pharmacother 96: 165-172, 2017.
20. Li C, Zhang Y, Zhao W, Cui S and Song Y: miR-153-3p regulates progression of ovarian carcinoma in vitro and in vivo by targeting MCL1 gene. J Cell Biochem 120: 19147-19158, 2019.
21. Wang T, Zhai M, Xu S, Ponnusamy M, Huang Y, Liu CY, Wang M, Shan C, Shan PP, Gao XQ, *et al*: NFATc3-dependent expression of miR-153-3p promotes mitochondrial fragmentation in cardiac hypertrophy by impairing mitofusin-1 expression. Theranostics 10: 553-566, 2020.
22. Canzio D and Maniatis T: The generation of a protocadherin cell-surface recognition code for neural circuit assembly. Curr Opin Neurobiol 59: 213-220, 2019.
23. Goodman KM, Rubinstein R, Dan H, Bahna F, Mannepalli S, Ahlsén G, Aye Thu C, Sampogna RV, Maniatis T, Honig B, *et al*: Protocadherin cis-dimer architecture and recognition unit diversity. Proc Natl Acad Sci USA 114: E9829-E9837, 2017.
24. Strehl S, Glatt K, Liu QM, Glatt H and Lalande M: Characterization of two novel protocadherins (PCDH8 and PCDH9) localized on human chromosome 13 and mouse chromosome 14. Genomics 53: 81-89, 1998.
25. Frank M, Ebert M, Shan W, Phillips GR, Arndt K, Colman DR and Kemler R: Differential expression of individual gamma-protocadherins during mouse brain development. Mol Cell Neurosci 29: 603-616, 2005.
26. Hirayama T and Yagi T: Regulation of clustered protocadherin genes in individual neurons. Semin Cell Dev Biol 69: 122-130, 2017.
27. Weng J, Xiao J, Mi Y, Fang X, Sun Y, Li S, Qin Z, Li X, Liu T, Zhao S, *et al*: PCDHGA9 acts as a tumor suppressor to induce tumor cell apoptosis and autophagy and inhibit the EMT process in human gastric cancer. Cell Death Dis 9: 27, 2018.
28. Weng J, Li S, Lin H, Mei H, Liu Y, Xiao C, Zhu Z, Cai W, Ding X, Mi Y, *et al*: PCDHGA9 represses epithelial-mesenchymal transition and metastatic potential in gastric cancer cells by reducing β-catenin transcriptional activity. Cell Death Dis 11: 206, 2020.
29. Livak KJ and Schmittgen TD: Analysis of relative gene expression data using real-time quantitative PCR and the $2^{-\Delta\Delta CT}$ method. *μ*ethods 25: 402-408, 2001.
30. Chiang HR, Schoenfeld LW, Ruby JG, Auyeung VC, Spies N, Baek D, Johnston WK, Russ C, Luo S, Babiarz JE, *et al*: Mammalian microRNAs: Experimental evaluation of novel and previously annotated genes. Genes Dev 24: 992-1009, 2010.
31. Li JH, Liu S, Zhou H, Qu LH and Yang JH: starBase v2.0: Decoding miRNA-ceRNA, miRNA-ncRNA and protein-RNA interaction networks from large-scale CLIP-Seq data. Nucleic Acids Res 42: D92-D97, 2014.
32. Chandrashekar DS, Bashel B, Balasubramanya SA, Creighton CJ, Ponce-Rodriguez I, Chakravarthi BV and Varambally S: UALCAN: A portal for facilitating tumor subgroup gene expression and survival analyses. Neoplasia 19: 649-658, 2017.
33. Pontén F, Jirström K and Uhlen M: The Human Protein Atlas - a tool for pathology. J Pathol 216: 387-393, 2008.
34. Jamal-Hanjani M, Wilson GA, McGranahan N, Birkbak NJ, Watkins TB, Veeriah S, Shafi S, Johnson DH, Mitter R, Rosenthal R, *et al*; TRACERx Consortium: Tracking the evolution of non-small-cell lung cancer. N Engl J Med 376: 2109-2121, 2017.
35. Blandin Knight S, Crosbie PA, Balata H, Chudziak J, Hussell T and Dive C: Progress and prospects of early detection in lung cancer. Open Biol 7: 170070, 2017.
36. Tulchinsky E, Demidov O, Kriajevska M, Barlev NA and Imyanitov E: EMT: A mechanism for escape from EGFR-targeted therapy in lung cancer. Biochim Biophys Acta Rev Cancer 1871: 29-39, 2019.
37. Otsuki Y, Saya H and Arima Y: Prospects for new lung cancer treatments that target EMT signaling. Dev Dyn 247: 462-472, 2018.
38. Zhang X, Sai B, Wang F, Wang L, Wang Y, Zheng L, Li G, Tang J and Xiang J: Hypoxic BMSC-derived exosomal miRNAs promote metastasis of lung cancer cells via STAT3-induced EMT. Mol Cancer 18: 40, 2019.
39. Zhong W, Yang W, Qin Y, Gu W, Xue Y, Tang Y, Xu H, Wang H, Zhang C, Wang C, *et al*: 6-Gingerol stabilized the p-VEGFR2/VE-cadherin/β-catenin/actin complex promotes microvessel normalization and suppresses tumor progression. J Exp Clin Cancer Res 38: 285, 2019.
40. Xiao T, Zhong W, Zhao J, Qian B, Liu H, Chen S, Qiao K, Lei Y, Zong S, Wang H, *et al*: Polyphyllin I suppresses the formation of vasculogenic mimicry via Twist1/VE-cadherin pathway. Cell Death Dis 9: 906, 2018.
41. Zhang Q, Li X, Li X, Li X and Chen Z: LncRNA H19 promotes epithelial-mesenchymal transition (EMT) by targeting miR-484 in human lung cancer cells. J Cell Biochem 119: 4447-4457, 2018.
42. Gong W, Su Y, Liu Y, Sun P and Wang X: Long non-coding RNA Linc00662 promotes cell invasion and contributes to cancer stem cell-like phenotypes in lung cancer cells. J Biochem 164: 461-469, 2018.
43. Bartl J, Forget A, Zanini M, Picard D, Qin N, Borkhardt A, Reifenberger G, Ayrault O and Remke M: SIG-03. HHIP-AS1 promotes tumor survival through stabilizing dynein Complex 1 in hedgehog driven human brain tumors. Neuro Oncol 21 (Suppl 2): ii113-ii114, 2019.
44. Ma R, Wang C, Wang J, Wang D and Xu J: miRNA-mRNA interaction network in non-small cell lung cancer. Interdiscip Sci 8: 209-219, 2016.
45. Agarwal V, Bell GW, Nam JW and Bartel DP: Predicting effective microRNA target sites in mammalian mRNAs. Elife 4: e05005, 2015.
46. Bartl J, Picard D, Borkhardt A, Reifenberger G and Remke M: Targeting the long non-coding RNA HHIP-AS1 in sonic hedgehog driven brain tumors. Klin Padiatr 228: A5, 2016.
47. Wang H, Zhong W, Zhao J, Zhang H, Zhang Q, Liang Y, Chen S, Liu H, Zong S, Tian Y, *et al*: Oleanolic acid inhibits epithelial-mesenchymal transition of hepatocellular carcinoma by promoting iNOS dimerization. Mol Cancer Ther 18: 62-74, 2019.
48. Chiou G-Y, Cherng J-Y, Hsu H-S, Wang ML, Tsai CM, Lu KH, Chien Y, Hung SC, Chen YW, Wong CI, *et al*: Cationic polyurethanes-short branch PEI-mediated delivery of Mir145 inhibited epithelial-mesenchymal transdifferentiation and cancer stem-like properties and in lung adenocarcinoma. J Control Release 159: 240-250, 2012.